



Effects of Joule Heating and Slip on Magnetohydrodynamics Hybrid Carbon Nanotubes Flow Through a Permeable Moving Plate

Nur Adilah Liyana Aladdin^{1,*}, Nur Syazana Anuar², Norfifah Bachok³, Farhan Ali⁴

¹ Department of Mathematics, Centre for Foundation Defence Studies, Universiti Pertahanan Nasional Malaysia, Kem Sg Besi, 57000 Kuala Lumpur, Malaysia

² School of Mathematical Sciences, College of Computing, Informatics and Mathematics, Universiti Teknologi MARA, 40450 Shah Alam, Selangor, Malaysia

³ Department of Mathematics and Statistics, Faculty of Science, Universiti Putra Malaysia, 43400 Serdang, Malaysia

⁴ Faculty of Computing and Information Technology, Indus University, Gulshan-e-Iqbal Karachi, 75300 Karachi, Pakistan

ARTICLE INFO

Article history:

Received 20 June 2024

Received in revised form 31 August 2024

Accepted 29 September 2024

Available online 31 October 2024

Keywords:

MHD; hybrid carbon nanotubes; slip velocity; joule heating; moving plate

ABSTRACT

The remarkable enhancement of heat transfer achieved by carbon nanotubes has motivated researchers to investigate further combinations with various working fluids. This research delves into elucidating the magnetohydrodynamics (MHD) flow characteristics of hybrid carbon nanotubes over a permeable moving plate while considering the influence of Joule heating and slip velocity. The combination of single-walled carbon nanotubes (SWCNT) and multi-walled carbon nanotubes (MWCNT) with water is employed for the analysis. The plate is expected to move either parallel or opposite to the free stream. Employing a similarity transformation, the governing equations are converted into a set of ordinary differential equations (ODEs). These ODEs are subsequently solved using the *bvp4c* solver within the MATLAB 2019a software package. In this problem, two solutions are obtained when considering the added effects. The 1% hybrid nanofluid fastens the separation of the boundary layer. However, the strengthening of 2% MHD and 40% slip velocity seem to slow down the separation of the boundary layer. The heat transfer rate is found to increase with elevated suction, magnetic field and volume fractions. The boundary layer thickness in heat transfer is broadened as the volume of nanoparticles increases from 2% to 4%. The Eckert numbers show that there is no significant effect on the heat transfer rate performance. These findings are new original and offer valuable insights for those engaged in related fields.

1. Introduction

The field of fluid dynamics has witnessed remarkable advancements, particularly in the realm of nanotechnology industries. This journey commenced with a focus on viscous fluids and has evolved into the exploration of nanofluids as discovered by Choi [1]. Nanofluids are characterized by the dispersion of smallest dimension nanoparticles into the base fluid, which in turn exhibit

* Corresponding author.

E-mail address: nuradilah@upnm.edu.my

<https://doi.org/10.37934/armne.24.1.5266>

commendable thermophysical properties. Rao [2] conducted a thorough investigation, delving into colloidal stability, diverse nanofluid phases and their rheological properties relevant to applications, highlighting their versatile applicability in electronics and nanotechnologies. Research findings consistently highlight the enhancement of heat transfer performance due to the presence of nanoparticles in fluids, with nanoparticle types ranging from oxides and carbides to metals and carbon nanotubes (CNTs).

Carbon nanotubes, including both multi-wall (MWCNTs) and single-wall (SWCNTs) variants, have been crucial in driving the revolutionary changes in nanotechnology industries. A study by Radushkevich and Lukyanovich [3] explored the groundwork of multi-walled carbon nanotubes (MWCNTs). Later, Iijima [4] unveiled the existence of helically structured microtubules composed of graphitic carbon. Iijima and Ichihashi [5] shared their findings on single-walled carbon nanotubes (SWCNTs). Presently, researchers continue to delve into understanding the unique characteristics of CNTs and their implications in boundary layer flow and heat transfer. In a flow model, both SWCNTs and MWCNTs were introduced into water, revealing that MWCNT yielded excellent results with the lowest thermal capacity and highest heat transfer compared to other nanofluids. Samat *et al.*, [6] conducted the problem over a moving plate in the presence of MHD. They employed the bvp4c to attain the skin friction and heat transfer rate. Ferdows *et al.*, [7] examined the uniform heat flux over a flat moving plate. Both studies agreed that SWCNT possesses a higher heat transfer rate compared to MWCNT. Meanwhile, Asshaari *et al.*, [8] added the effect of Brownian and thermophoresis using the same nanoparticles. They found that the increasing volume fraction, Brownian and thermophoresis reduce the heat transfer. However, an increase in mass transfer rate was observed due to the impeded movement of the nanoparticles in the boundary layer flow.

Today, hybrid nanofluid emerges as a favourable option among researchers, representing an innovative class that combines multiple types of nanoparticles with a base fluid to enhance its properties. This fluid employs a synergistic approach to boost thermal and fluidic properties. Furthermore, it demonstrates superior heat transfer capabilities compared to conventional nanofluids, leveraging the unique characteristics of various nanoparticle types. Researchers are actively exploring the synthesis, properties and applications of hybrid nanofluids to unlock their full potential in optimizing thermal management and energy efficiency. The influence of the shape factor of hybrid nanoparticles (SWCNT-MWCNT) on the convective heat and mass transfer of two immiscible fluids in an inclined duct, by employing the perturbation technique was done by Ananth *et al.*, [9]. In their study, three different shapes of nanoparticles which are brick, blade and lamina were considered. Lamina shape has better performance and giving a significant effect on the Soret number. Meanwhile, Khashi'ie *et al.*, [10] highlight the findings that the heat transfer rate using blade shape is dominant compared to spherical shape for hybrid nanofluid Cu - Al₂O₃/water over a radiative EMHD plate. Roy and Akter [11] studied in mixed convective of Cu - Al₂O₃/water over a shrinking cylinder saturated in a porous medium. To date, numerous researchers have come out with theoretical works on hybrid nanofluid.

In the domain of fluid dynamics, the slip effect characterizes the relative motion between a fluid and a solid surface in contact, deviating from the conventional no-slip boundary condition. Traditionally, the no-slip condition asserts that the fluid velocity at the solid surface aligns with the velocity of the surface itself. However, practical scenarios reveal slip effects when a tangential velocity difference arises between the fluid and the solid boundary. The exploration of slip effects extends to specific studies in hybrid nanofluid dynamics. Kumar [12] investigated the slip effect in the context of hybrid nanofluid flow over a stretching cylinder. Addressing a moving thin needle, Kirusakhtika *et al.*, [13] utilized Fe₃O₄ + Al₂O₃/water to solve the associated problem. Meanwhile, Najib *et al.*, [14] tackled the unsteady hybrid nanofluid dynamics using bvp4c MATLAB, a dual solution

that appeared within a certain parameter range. Additional contributions on slip effects have been documented by [15-17].

Magnetohydrodynamics (MHD) explores the behaviour of electrically conductive fluids under the influence of magnetic fields. The conductive fluids are liquid metals, plasmas and ionized gases. The interaction between magnetic fields and these conductive fluids gives rise to distinctive phenomena and intricate dynamics. This distinctiveness stems from the capacity of magnetic fields to exert a drag force, referred to as the Lorentz force, which can hinder fluid motion while simultaneously altering the fluid's temperature and concentration. Hartmann [18] introduced the theory of laminar flow in an electrically conductive fluid subjected to a homogeneous magnetic field. This contribution laid the foundation for extensive research in MHD over the past few decades. Researchers have adopted the use of MHD in their theoretical work due to the widely used of MHD in industrial. Alqahtani *et al.*, [19] examined the role of viscosity and aggregation of nanoparticles through MHD rotating flow. Sharma *et al.*, [20] exposed the findings in a micropolar fluid flow over a stretching surface. The work on MHD flow was continuously been studied by numerous researchers. Few literature series on MHD can be seen in [21-23].

Another effect that is always considered in boundary layer problems is Joule heating. It refers to the phenomenon where electrical energy is converted into heat energy within a conducting medium, typically due to the presence of an electric current. This effect is particularly relevant in fluid dynamics, especially in electroconvection or magnetohydrodynamics (MHD), where electric or magnetic fields influence the flow of electrically conductive fluids. Joule heating contributes to the temperature distribution within the medium, with regions experiencing higher heating exhibiting elevated temperatures, impacting the overall thermal behaviour of the system. The application of Joule heating can be seen in electrical heating devices, electronics, automotive industry, medical etc. Research done by Reddy and Reddy [24] reported the influence of Joule heating in nanofluid flow with compliant walls. They concurred that this control parameter is used to increase the nanofluid's temperature. Ibrahim and Gizewu [25] conducted a comprehensive study involving stability analysis and the investigation of dual solutions for the mixed convection and thermal radiation phenomena of hybrid nanofluid flow passing over a curved surface subjected to stretching or shrinking, with consideration for injection or suction conditions. The vertical problem involving Joule heating, viscous dissipation and energy activation was proposed by Jayanthi and Niranjana [26]. The following papers are also discussed on the effect of Joule heating through various surfaces [27-30].

However, this study aims to address the gap by theoretically and mathematically formulating the fluid model as well as analysing the selected governing parameters in controlling the skin friction, heat transfer, boundary layer separation and profiles of velocity and temperature, respectively. Since carbon nanotubes provide lots of advantages, this study opted the hybrid carbon nanotubes as the nanoparticles. Considering the effects of magnetohydrodynamic (MHD), Joule heating and slip which has not been worked out by aforementioned researchers. The novelties of this study are:

- i. Provides optimizing heat transfer rate of hybrid carbon nanotubes with simultaneous effects were added into the flow.
- ii. Construct a new mathematical modelling by considering MHD, Joule heating, suction and velocity slip effects.
- iii. Highlight the impact of MHD, Joule heating, suction and slip effects in hybrid carbon nanotube flow.
- iv. Therefore, this study aims to answer three main research questions:
 - What is the role of the governing parameters in determining the critical values for boundary layer separation and dual solution?

- How can the simultaneous effects of MHD, Joule heating and slip affect the flow behaviour, skin friction and heat transfer?
- Does the higher concentration of SWCNT-MWCNT/water enhance the boundary layer separation and heat transfer rate?

2. Formation of Problem

In this section, we present the formulation of the mathematical model of the flow together with the boundary conditions. The governing equations consist of three important equations which are: continuity, momentum and energy. The effects of MHD and Joule heating are incorporated in the momentum and energy equations, respectively. Meanwhile, the velocity slip effect is placed in the boundary conditions. Similarity transformation is adopted to reduce the partial differential equations (PDEs) of governing equations into ODEs. BVP4c MATLAB is used to compute numerically and plot the graphs for discussions.

2.1 Mathematical Modelling

Initially, consider a two-dimensional steady boundary layer of a hybrid carbon nanotube slip flow through a permeable moving plate with the effects of MHD and Joule heating. Figure 1 illustrates that the fluid flow occupied at the x and y axes (i.e.: $x, y \geq 0$). This physical model relies on a few assumptions:

- i. The x -axis is aligned to the plate's surface while the y -axis is the coordinate measured normal to it.
- ii. Single wall carbon nanotubes (SWCNT) and multi-wall carbon nanotubes are chosen with concentrations of 1% - 3%. The hybrid carbon nanotubes are formed by dispersing in water as the base fluid. The thermophysical properties following Anuar *et al.*, [33] are tabulated in Table 1, while the values for each of the properties are furnished in Table 2.
- iii. The hybrid carbon nanotubes are said to be in thermal equilibrium.
- iv. It is assumed that the temperature at the plate is denoted by T_w , while the temperature of the surrounding ambient fluid is denoted by T_∞ .
- v. λ acts as the moving plate parameter. If either moving away from the origin ($\lambda > 0$) or to the origin ($\lambda < 0$), respectively.
- vi. The last term in Eq. (2) represents the x -component of the magnetic field. The magnetic field, which generates the magnetohydrodynamics effect with constant, B where $B = B_0(2x)^{-1/2}$ following Aladdin *et al.*, [34]. In this study, we have disregarded the induced magnetic field due to the magnetic number of Reynolds, R_m is assumed to be very small.
- vii. The last term in Eq. (3) signifies the Joule heating effects. are added simultaneously to the flow. Incorporating Joule heating is significant due to the presence of MHD which will electrically interact with each other.
- viii. The velocity slip effect is denoted by L which will modify the velocity boundary at the surface, allowing for partial fluid adherence. Incorporating the mass fluid velocity, $V_w = -(Uv_f/2x)^{1/2}S$ where $V_w > 0$ (suction) and $V_w < 0$ (injection). The impermeable surface is characterized when $V_w = 0$.

In light of the above assumptions, the governing equations consist of continuity, momentum and energy equations (1) – (3) were set up following the work from Devi and Devi [31] and Khashi'ie *et al.*, [32].

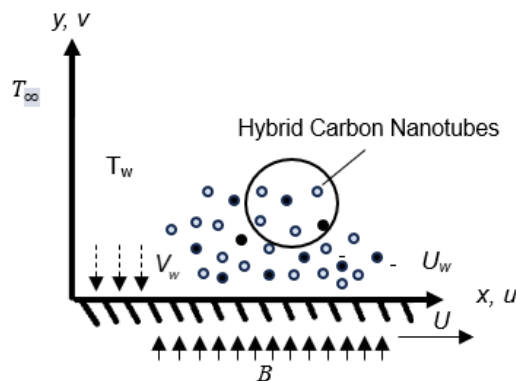


Fig. 1. Illustration of physical model with coordinate system

$$\frac{\partial u}{\partial x} + \frac{\partial v}{\partial y} = 0 \quad (1)$$

$$u \frac{\partial u}{\partial x} + v \frac{\partial u}{\partial y} = \frac{\mu_{hnf}}{\rho_{hnf}} \frac{\partial^2 u}{\partial y^2} - \frac{\sigma_{hnf}}{\rho_{hnf}} B^2 (u - U) \quad (2)$$

$$u \frac{\partial T}{\partial x} + v \frac{\partial T}{\partial y} = \alpha_{hnf} \frac{\partial^2 T}{\partial y^2} + \frac{\sigma_{hnf}}{\rho_{hnf}} B^2 (u - U)^2 \quad (3)$$

And the boundary conditions (BCs):

$$\begin{aligned} u &= \lambda U + L \frac{\partial u}{\partial y}, \quad v = V_w, \quad T = T_w \quad \text{at } y = 0 \\ u &\rightarrow U, \quad T \rightarrow T_\infty \quad \text{at } y \rightarrow \infty \end{aligned} \quad (4)$$

2.2 Thermophysical Properties of Hybrid Carbon Nanotubes

Devi and Devi [31] utilized the thermophysical properties of hybrid nanofluids in their investigation of a stretching sheet, incorporating various flow effects. Nevertheless, a notable distinction in thermal conductivity arises when hybrid carbon nanotubes are introduced. Following Anuar *et al.*, [34] employed the modified Maxwell model contributes to the thermal conductivity correlation as presented in Table 1 together with the other thermophysical properties of hybrid carbon nanotubes. Besides, a few assumptions are acknowledged in this study:

- i. Nanoparticle shape is assumed to be uniform and spherical.
- ii. Nanoparticles are considered to be in thermal equilibrium.
- iii. The combination of nanoparticles is assumed to be stable.

Table 1
 Correlation on hybrid carbon nanotubes thermophysical properties [34]

Thermophysical	Hybrid carbon nanotubes
Density	$\rho_{hnf} = (1 - \varphi_2)[(1 - \varphi_1)\rho_f + \varphi_1\rho_{s1}] + \varphi_2\rho_{s2}$
Heat capacity	$(\rho C_p)_{hnf} = (1 - \varphi_2) [(1 - \varphi_1)(\rho C_p)_f + \varphi_1(\rho C_p)_{s1}] + \varphi_2(\rho C_p)_{s2}$
Viscosity	$\mu_{hnf} = \frac{\mu_f}{(1 - \varphi_1)^{2.5}(1 - \varphi_2)^{2.5}}$
Thermal conductivity	$k_{hnf} = \left[\frac{1 - \varphi_2 + 2\varphi_2 \left(\frac{k_s}{k_s - k_{nf}} \right) \ln \left(\frac{k_s + k_{nf}}{2k_{nf}} \right)}{1 - \varphi_2 + 2\varphi_2 \left(\frac{k_{nf}}{k_s - k_{nf}} \right) \ln \left(\frac{k_s + k_{nf}}{2k_{nf}} \right)} \right] k_{nf}$
	$k_{nf} = \left[\frac{k_{s1} + 2k_f - 2\varphi_1(k_f - k_{s1})}{k_{s1} + 2k_f + \varphi_1(k_f - k_{s1})} \right] k_f$
Electrical conductivity	$\sigma_{hnf} = \left[\frac{\sigma_{s2} + 2\sigma_{nf} - 2\varphi_2(\sigma_{nf} - \sigma_{s2})}{\sigma_{s2} + 2\sigma_{nf} + \varphi_2(\sigma_{nf} - \sigma_{s2})} \right] \sigma_{nf}$
	$\sigma_{nf} = \left[\frac{\sigma_{s2} + 2\sigma_{nf} - 2\varphi_1(\sigma_f - \sigma_{s1})}{\sigma_{s1} + 2\sigma_f + \varphi_1(\sigma_f - \sigma_{s1})} \right] \sigma_f$

The subscripts f , nf and hnf denote three types of fluids: viscous fluid, nanofluid and hybrid nanofluids, respectively. Additionally, φ_1 and φ_2 represent the volume fractions of two distinct nanoparticles, corresponding to SWCNT and MWCNT. Furthermore, $s1$ and $s2$ refer to the solid nanoparticles associated with SWCNT and MWCNT, respectively. To maintain consistency with these correlations, the assumptions $S = s1 + s2$ and $\varphi = \varphi_1 + \varphi_2$ were incorporated. In this study, 1% SWCNT is added consistently to 2% and 3% MWCNT into water to form a hybrid carbon nanotube. It is also important to highlight the values of the thermophysical property for SWCNT, MWCNT and water. A comprehensive listing of the values was tabulated in Table 2.

Table 2
 Numerical values for thermophysical properties

Thermophysical Properties	k (W/mK)	C_p (J/kgK)	ρ (kg/m ³)	σ (s/m)
SWCNT	6600	425	2600	1x10 ⁶
MWCNT	3000	796	1600	1x10 ⁷
Water	0.613	4179	997	5.5x10 ⁻⁶

2.3 Similarity Solution

Solving complex non-linear partial differential equations is difficult and tedious. Thus, we introduce a similarity transformation, to reduce the multiple independent variables in the PDEs to n ODEs with simple variables. Based on the boundary layer flow geometries and its boundary conditions, we proposed a stream function, ψ where $u = \frac{\partial \psi}{\partial y}$ and $v = -\frac{\partial \psi}{\partial x}$. The following similarity solutions are presented below: (Khashi'ie *et al.*, [32])

$$\eta = y \left(\frac{U}{2v_f x} \right)^{1/2}, \quad \psi = (2v_f x U)^{1/2} f(\eta), \quad T - T_\infty = (T_w - T_\infty)\theta(\eta)$$

$$u = U f'(\eta), \quad v = \left(\frac{U v_f}{2x} \right)^{1/2} [\eta f'(\eta) - f(\eta)] \tag{5}$$

Differentiate Eq. (5) with respect to the variables involved in Eq. (1) to Eq. (4). Eq. (1) satisfied for both sides of the equations. Eq. (2) to Eq. (4) are transformed into ODEs of momentum and energy equation:

$$\left(\frac{\mu_{hnf}/\mu_f}{\rho_{hnf}/\rho_f}\right) f''' + f f'' - \left(\frac{\sigma_{hnf}/\sigma_f}{\rho_{hnf}/\rho_f}\right) M(f' - 1) = 0 \quad (6)$$

$$\frac{1}{Pr} \frac{k_{hnf}/k_f}{(\rho C_p)_{hnf}/(\rho C_p)_f} \theta'' + f \theta' + \left(\frac{\sigma_{hnf}/\sigma_f}{\rho_{hnf}/\rho_f}\right) MEc(f' - 1)^2 = 0 \quad (7)$$

together with BCs:

$$\left. \begin{aligned} f(0) = S, \quad f'(0) = \lambda + \sigma_L f''(0), \quad \theta(0) = 1 \\ f'(\eta) \rightarrow 1, \theta(\eta) \rightarrow 0 \end{aligned} \right\} \quad (8)$$

where the dimensionless parameters in Eq. (6) to Eq. (8) are defined as Prandtl number, magnetic field, Eckert number and the slip velocity parameters as follows:

$$Pr = \frac{(\mu C_p)_f}{k_f}, \quad M = \frac{B_0^2 \sigma_f}{U \rho_f}, \quad Ec = \frac{U^2}{(C_p)_f (T_w - T_\infty)}, \quad \sigma_L = L \left(\frac{U}{2xv_f}\right)^{1/2} \quad (9)$$

The physical quantities interest which fulfil the objectives of this study are skin friction coefficient, C_f and the local Nusselt number, Nu_x defined as,

$$C_f = \frac{\mu_{hnf}}{U^2 \rho_f} \left(\frac{\partial u}{\partial y}\right)_{y=0}, \quad Nu_x = -\frac{x k_{hnf}}{k_f (T_w - T_\infty)} \left(\frac{\partial T}{\partial y}\right)_{y=0} \quad (10)$$

By employing Eq. (5) into Eq. (10), the reduced form of skin friction coefficient and heat transfer are:

$$\sqrt{2} Re_x^{1/2} C_f = \frac{\mu_{hnf}}{\mu_f} f''(0), \quad \sqrt{2} Re_x^{-1/2} Nu_x = -\frac{k_{hnf}}{k_f} \theta'(0) \quad (11)$$

where $Re_x = Ux/v_f$.

3. Results and Discussion

Numerical computations are conducted for various values of the parameters such as M , λ , Ec , φ and σ_L aiming in providing a comprehensive insight into the problem. The parameter ranges are defined as follows: $M(0 \leq M \leq 0.02)$, $Ec(0.01 \leq Ec \leq 1)$, $\sigma_L (0 \leq \sigma_L \leq 0.4)$ and $\varphi_1(0 \leq \varphi_1 \leq 0.03)$ while maintaining a constant value for $Pr = 6.2$. Eq. (6) to Eq. (8) are solved numerically using the `bvp4c` solver in MATLAB, which employs the finite difference method. It necessitates the specification of an initial guess at the initial mesh point and adjustment of the step size to achieve the desired accuracy. Before generating further results, a validation test was made with previous similar finding from aforementioned by Khan *et al.*, [35] to authenticate the accuracy of the present model.

Throughout the computation, dual solutions have appeared in a certain range of parameters. Since the discussion on the nature of the dual solution has been published by numerous researchers,

this paper will focus on the skin friction, local Nusselt number as well as the profile of velocity and temperature. For the validation, Table 3 outlined the data produced by the present model for $M = S = Ec = \sigma_L = 0$ at $\eta \approx 20$. Both results are compatible and in a very good consensus.

Table 3
 Comparison of skin friction, $f''(0)$ when $M = S = Ec = \sigma_L = 0$

φ_1	φ_2	λ	Khan <i>et al.</i> , [35]	Present	
				First solution	Second solution
0	0	0	0.4696	0.4696	
0	0.01	-0.25		0.3977	0.0449
		-0.15		0.4448	0.0086
		0		0.4651	
		0.2		0.4389	
0.01	0.01	-0.25		0.3958	0.0447
		-0.15		0.4427	0.0085
		0		0.4629	
		0.2		0.4369	

Figure 2 and Figure 3 portray the result of $\sqrt{2}C_f Re_x^{1/2}$ and $\sqrt{2}Nu_x Re_x^{-1/2}$ for three types of fluid which are viscous fluid ($\varphi_1 = \varphi_2 = 0$), SWCNT/water ($\varphi_1 = 0.01, \varphi_2 = 0$) and SWCNT-MWCNT/water ($\varphi_1 = 0.01, \varphi_2 = 0.01$). Notably, the presence of hybrid carbon nanotubes is observed to expedite the reduction of the boundary layer separation. Furthermore, the dual solutions are observed to emerge when $\lambda < 0$, indicating the flow in opposing directions. No solution is identified for $\lambda < \lambda_c$. Apart from that, an increase in φ_1 and φ_2 , resulting a decrease pattern of skin friction and an enhancement of the heat transfer rate at the surface.

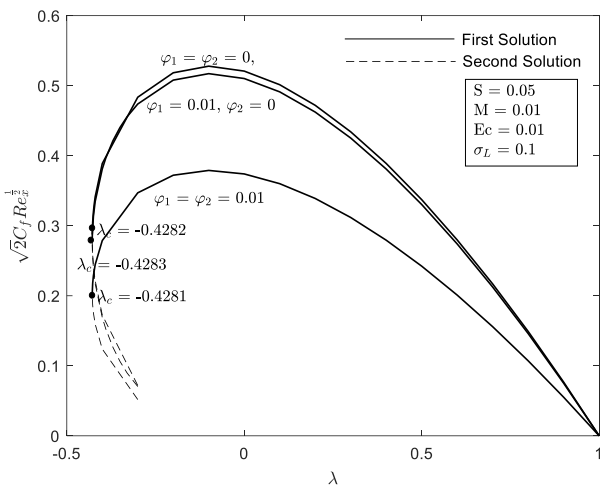


Fig. 2. Distribution of skin friction coefficient with three distinct types of fluid and λ

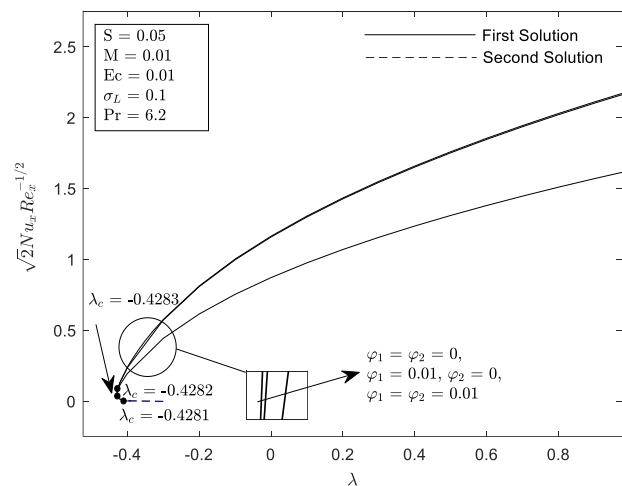


Fig. 3. Distribution of heat transfer coefficient with three distinct types of fluid and λ

Figure 4 and Figure 5 depict the distribution of $\sqrt{2}C_f Re_x^{1/2}$ and $\sqrt{2}Nu_x Re_x^{-1/2}$ for various values of M . As M increases, there is a consistent decrease in the values of both the skin friction coefficient and the heat transfer coefficient. This behaviour is linked to the impact of the Lorentz force in the presence of a strengthened M , which tends to impede the motions of the fluid, resulting in a noticeable reduction in skin friction and temperature along the surface. The strengthening of the magnetic parameter induces a noticeable thinning of the boundary layer and implies that as M increases, the separation of the boundary layer becomes more rapid i.e.: $M = 0$ ($\lambda_c = -0.3765$), $M = 0.01$ ($\lambda_c = -$

0.3945) and $M = 0.02$ ($\lambda_c = -0.4128$). The graph indicates that dual solutions occur when $\lambda_c < 0$, a unique solution emerges for $\lambda > 0$ and no solution is found for $\lambda < \lambda_c$. This highlights the intricate relationship among the magnetic parameter, flow properties and thermal distribution within magnetohydrodynamic flows.

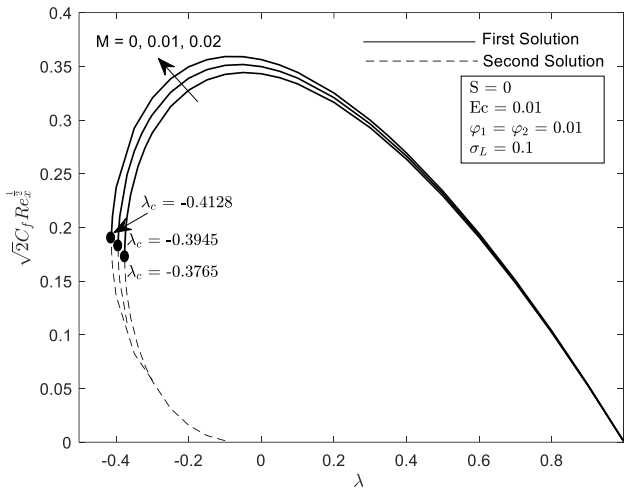


Fig. 4. Distribution of skin friction coefficient with several values of M and λ

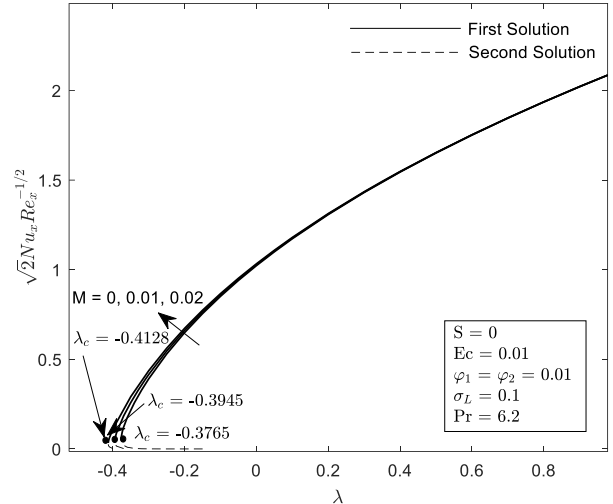


Fig. 5. Distribution of heat transfer coefficient with several values of M and λ

Further observation of the effect of slip parameters can be seen in Figure 6 and Figure 7. When there is no-slip condition ($\sigma_L = 0$), the similarity solution exists at $\lambda_c = -0.3712$. The range of λ increase as the slip parameter increases by 2%, i.e.: $\sigma_L = 0.02$ ($\lambda_c = -0.4197$) and $\sigma_L = 0.04$ ($\lambda_c = -0.4754$). Generally, the slip parameter affects the drag force experienced by the fluid. An increase in slip may reduce the drag force owing to the relative motion between the fluid and the solid surface which can be seen that there is a turning point at each of the slip effect. This alteration can potentially modify the thermal boundary layer, thereby influencing the heat transfer rate between the fluid and the solid surface.

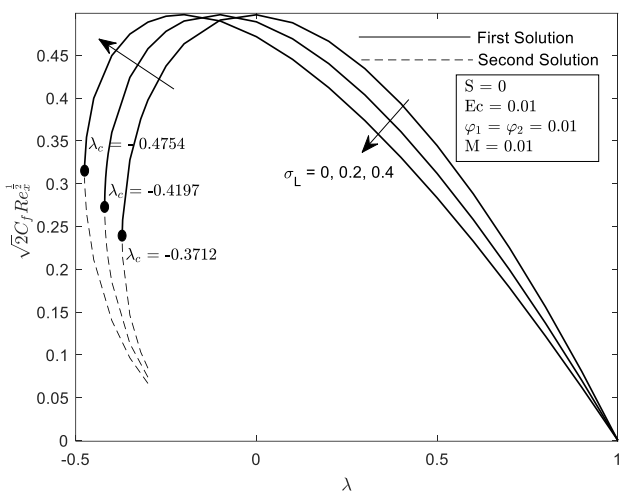


Fig. 6. Distribution of skin friction coefficient with several values of σ_L and λ

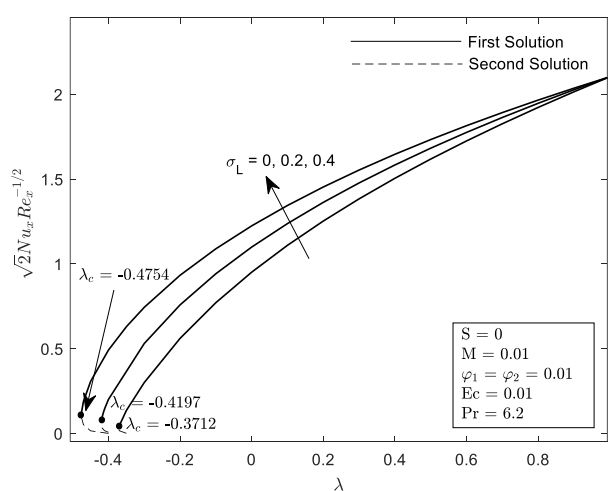


Fig. 7. Distribution of heat transfer coefficient with several values of σ_L and λ

Figure 8 highlights the distribution $\sqrt{2}Nu_x Re_x^{-1/2}$ with several Eckert number ($Ec = 0, 0.01, 1$). In this figure we are considering the graph of heat transfer rate as the term only appears in Eq. (6). The

Eckert number has a notable impact on heat transfer. The expression of the Eckert number is derived from the combination of Joule heating and magnetic field. The intense of Eckert number reduced the heat transfer rate and thinning the range of solution. However, it does not affect the separation of the boundary layer ($\lambda_c = -0.3945$). The high Eckert number indicates that there is a substantial kinetic energy component, where the heat transfer may be more influenced by convective processes. Conversely, lower Ec suggests a stronger influence of internal energy and heat transfer may be dominated by conductive or convective mechanisms, depending on the specific conditions. A higher Ec indicates a greater dominance of kinetic energy relative to internal energy. This distinction is particularly relevant in situations characterized by significant kinetic energy, such as in fast-flowing conditions. Moreover, the elevation in kinetic energy results in an increase in fluid temperature, as depicted in Figure 9. This is due to the fact that a greater proportion of the energy is linked to the fluid's motion, resulting in an elevation of internal energy and consequently an increase in temperature.

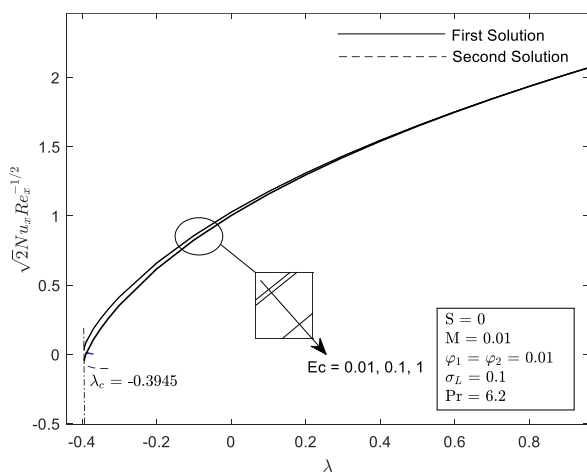


Fig. 8. Distribution of heat transfer coefficient with several values of Ec and λ

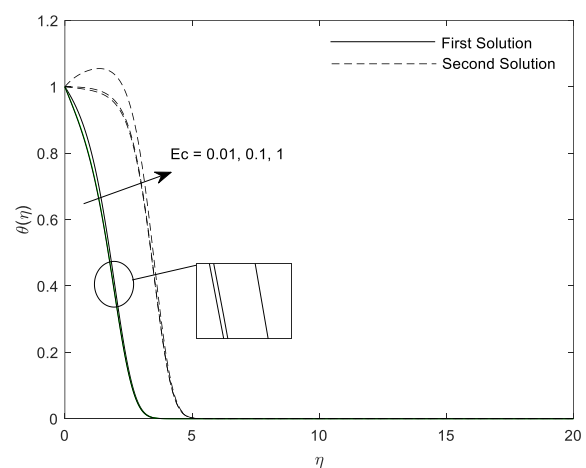


Fig. 9. Temperature profile with several values of Ec

Figure 10 and Figure 11 present the distribution of $\sqrt{2}C_f Re_x^{1/2}$ and $\sqrt{2}Nu_x Re_x^{-1/2}$ for M with φ . The magnetic parameter, M and the volume fraction nanoparticles φ increase simultaneously. A higher magnetic parameter generally implies a stronger magnetic field. In MHD flows, a strong magnetic field can suppress fluid motion due to the Lorentz force. On top of that, it will lead to a strong shear stress in the skin friction which will reduce the velocity gradients at the fluid-solid interface. The magnetic parameter affects the thickness of the boundary layer near the solid surface. Higher M tends to thin the boundary layer, thereby affecting the velocity and temperature profiles which is explained in Figure 14 and Figure 15.

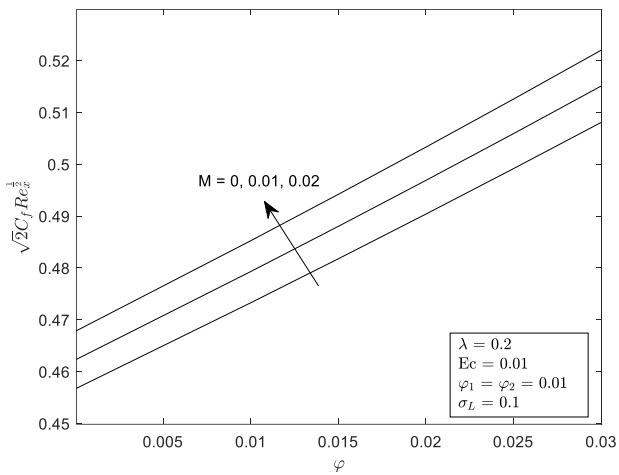


Fig. 10. Distribution of skin friction coefficient with several values of M and ϕ

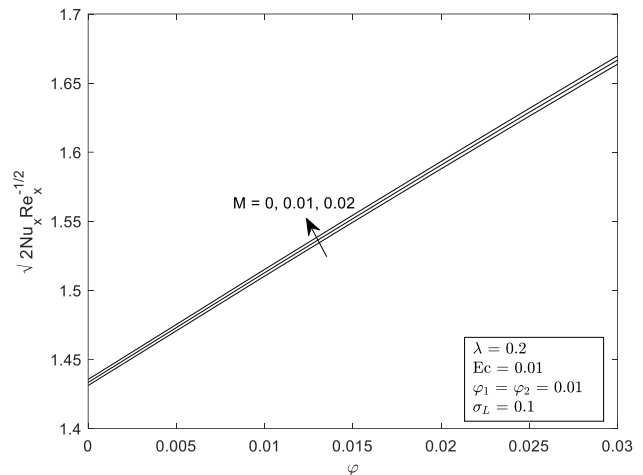


Fig. 11. Distribution of heat transfer coefficient with several values of M and ϕ

Meanwhile, Figure 12 and Figure 13 portray the distribution of $\sqrt{2}C_f Re_x^{1/2}$ and $\sqrt{2}Nu_x Re_x^{-1/2}$ for several values of ϕ_2 and ϕ_1 . Notably, the 2% hybrid carbon nanotubes with yield significantly higher results compared to the case where $\phi_2 = 0$. This improvement can be attributed to the presence of multiple concentrations of nanoparticles within the hybrid carbon nanotubes which might affect the thermophysical properties. These factors collectively contribute to a reduction in frictional forces among the layers of the fluid. The synergistic effect of the hybrid nanofluid's composition, characterized by diverse concentrations and densities, leads to an overall enhancement in the examined parameters. Furthermore, this improvement in skin friction coefficient extends to the enhancement of heat transfer characteristics. Perhaps, the boundary layer thickness in heat transfer expands widely as the volume increases by 2% and 4%. The interaction of these factors accentuates the potential of hybrid nanofluids to mitigate frictional effects and concurrently improve heat transfer rates in the fluid layers.

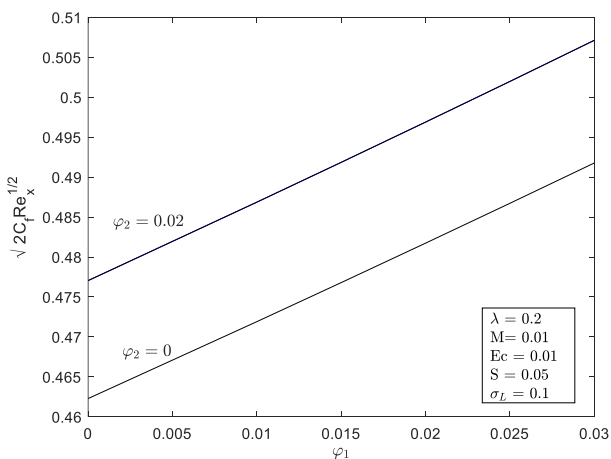


Fig. 12. Distribution of skin friction coefficient with several values of ϕ_2 and ϕ_1

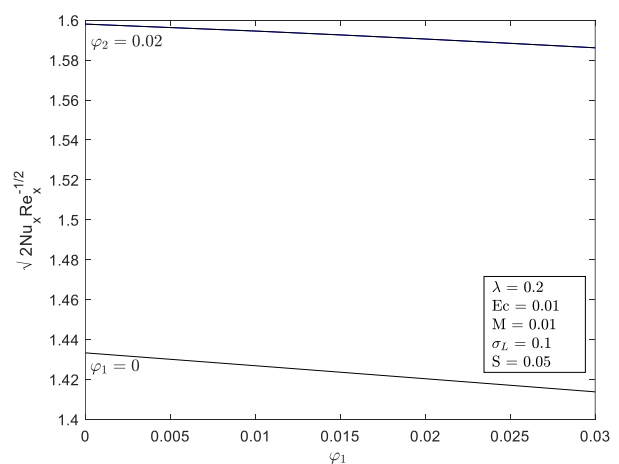


Fig. 13. Distribution of heat transfer coefficient with several values of ϕ_2 and ϕ_1

Table 4 reveals the distribution of $\sqrt{2}C_f Re_x^{1/2}$ and $\sqrt{2}Nu_x Re_x^{-1/2}$ for several values of suction. From the table, it is worth noting that the distribution of skin friction and heat transfer increases with the increase of the volume fraction nanoparticles. Generally, an increase in suction intensity corresponds to a greater extraction of mass from the laminar boundary layer through the permeable

walls. Simultaneously, an elevated value of S encourages the fluid to migrate towards unoccupied regions, impacting the surface limits. This shift results in heightened shear stress on the surface, triggering the emergence of φ and the generation of heat within the fluid. The ensuing heat contributes to an elevation in the fluid temperature, consequently empowering and promoting an enhanced fluid flow.

Table 4
 Distribution of skin friction, $\sqrt{2}C_f Re_x^{1/2}$ and heat transfer coefficient, $\sqrt{2}Nu_x Re_x^{-1/2}$ when $M = 0.01, Ec = 0.01, \sigma_L = 0.1$

S	φ	$\sqrt{2}C_f Re_x^{1/2}$	$\sqrt{2}Nu_x Re_x^{-1/2}$
0	0	0.4373	1.2277
	0.01	0.4537	1.3515
	0.02	0.4707	1.3919
	0.03	0.4884	1.4712
0.25	0	0.5647	2.3632
	0.01	0.5840	2.4199
	0.02	0.6039	2.4762
	0.03	0.6245	2.5319
0.5	0	0.6962	3.6848
	0.01	0.7187	3.7044
	0.02	0.7417	3.7257
	0.03	0.7652	3.7479

Figure 14 and Figure 15 portray the $f'(\eta)$ and $\theta(\eta)$ profiles for several values of M . The velocity of fluid decreases for both solutions. This indicates that the Lorentz force affects the surface and velocity of the fluid. Likewise, the temperature profile shows decreasing in the first solution and increasing in the second solution.

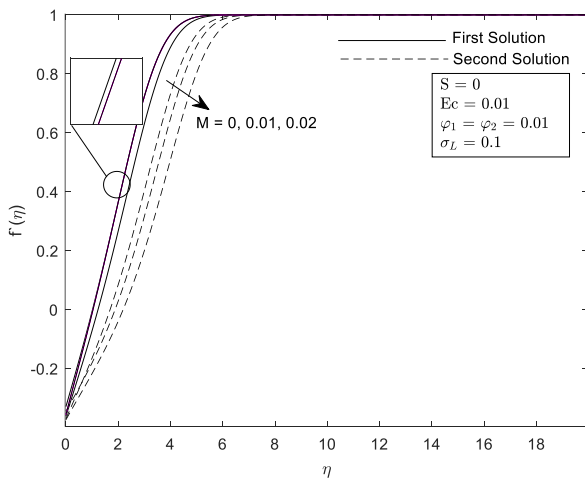


Fig. 14. Velocity profile for several M

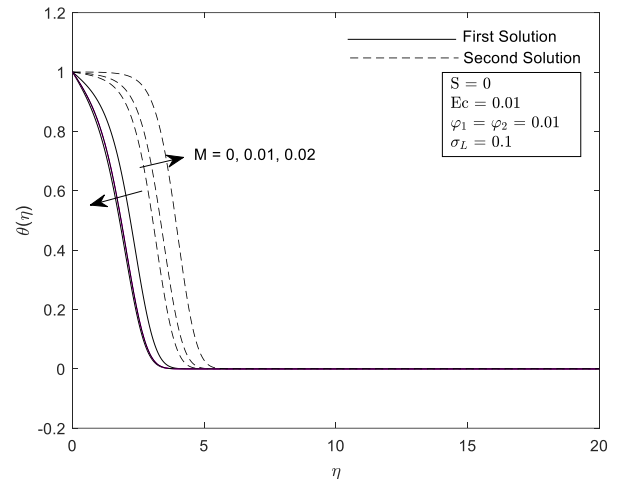


Fig. 15. Temperature profile for several M

4. Conclusion

A comprehensive examination in analysing the magnetohydrodynamics (MHD) hybrid carbon nanotubes' behaviour over a permeable moving plate, considering the influence of slip and Joule heating. The findings obtained from this investigation allow for conclusive insights into the research questions outlined in the earlier sections of the study:

- i. The existence of a dual solution is feasible at a certain range of parameters added.
- ii. The magnetic parameter increases the skin friction and the heat transfer rate as the value of M is prominent in the flow.
- iii. The increase of Joule heating reduces the heat transfer coefficient. However, the additional Eckert number does not significantly affect the boundary layer separation.
- iv. The slip and suction enhance the skin friction and heat transfer rate.
- v. The addition of a combination of SWCNT-MWCNT/water has increased the skin friction coefficient and heat transfer rate compared to SWCNT/water and viscous.

Acknowledgement

The authors wish to express their sincere appreciation to the reviewers for their thorough, supportive and insightful feedback on this manuscript. Furthermore, our gratitude extends to Universiti Pertahanan Nasional Malaysia for covering the technical fees and providing the MATLAB 2019a license.

References

- [1] Choi, S. US and Jeffrey A. Eastman. *Enhancing thermal conductivity of fluids with nanoparticles*. No. ANL/MSD/CP-84938; CONF-951135-29. Argonne National Lab.(ANL), Argonne, IL (United States), 1995.
- [2] Rao, Yuanqiao. "Nanofluids: stability, phase diagram, rheology and applications." *Particology* 8, no. 6 (2010): 549-555. <https://doi.org/10.1016/j.partic.2010.08.004>
- [3] Lukyanovich, V. M. R. L. V. "The structure of carbon forming in thermal decomposition of carbon monoxide on an iron catalyst." *Soviet Journal of Physical Chemistry* 26 (1952): 88-95.
- [4] Iijima, Sumio. "Helical microtubules of graphitic carbon." *nature* 354, no. 6348 (1991): 56-58. <https://doi.org/10.1038/354056a0>
- [5] Iijima, Sumio and Toshinari Ichihashi. "Single-shell carbon nanotubes of 1-nm diameter." *nature* 363, no. 6430 (1993): 603-605. <https://doi.org/10.1038/363603a0>
- [6] Samat, Nazrul Azlan Abdul, Norfifah Bachok and Norihan Md Arifin. "Carbon Nanotubes (CNTs) Nanofluids Flow and Heat Transfer under MHD Effect over a Moving Surface." *Journal of Advanced Research in Fluid Mechanics and Thermal Sciences* 103, no. 1 (2023): 165-178. <https://doi.org/10.37934/arfmts.103.1.165178>
- [7] Ferdows, M., Md Shamshuddin, Motahar Reza and Raushan Ara Quadir. "Heat transfer effects on carbon nanotubes along a moving flat plate subjected to uniform heat flux." *International Journal of Applied Mechanics and Engineering* 27, no. 4 (2022): 66-81. <https://doi.org/10.2478/ijame-2022-0051>
- [8] Asshaari, Izamarlina, Alias Jedi and Shahrir Abdullah. "Brownian motion and thermophoresis effects in co-flowing carbon nanotubes towards a moving plate." *Results in Physics* 44 (2023): 106165. <https://doi.org/10.1016/j.rinp.2022.106165>
- [9] Ananth Subray, P. V., B. N. Hanumagowda, S. V. K. Varma and Mohammad Hatami. "The impacts of shape factor and heat transfer on two-phase flow of nano and hybrid nanofluid in a saturated porous medium." *Scientific Reports* 12, no. 1 (2022): 21864. <https://doi.org/10.1038/s41598-022-26169-z>
- [10] Khashi'ie, Najiyah Safwa, Norihan Md Arifin, Mikhail Sheremet and Ioan Pop. "Shape factor effect of radiative Cu-Al₂O₃/H₂O hybrid nanofluid flow towards an EMHD plate." *Case Studies in Thermal Engineering* 26 (2021): 101199. <https://doi.org/10.1016/j.csite.2021.101199>
- [11] Roy, Nepal Chandra and Aysha Akter. "Dual solutions of mixed convective hybrid nanofluid flow over a shrinking cylinder placed in a porous medium." *Heliyon* 9, no. 11 (2023). <https://doi.org/10.1016/j.heliyon.2023.e22166>
- [12] Kumar, T. Sravan. "Hybrid nanofluid slip flow and heat transfer over a stretching surface." *Partial Differential Equations in Applied Mathematics* 4 (2021): 100070. <https://doi.org/10.1016/j.padiff.2021.100070>
- [13] Kirusakthika, S., S. Priya, AK Abdul Hakeem and B. Ganga. "MHD slip effects on (50: 50) hybrid nanofluid flow over a moving thin inclined needle with consequences of non-linear thermal radiation, viscous dissipation and inclined Lorentz force." *Mathematics and Computers in Simulation* 222 (2024): 50-66. <https://doi.org/10.1016/j.matcom.2023.07.015>
- [14] Najib, Najwa, Nor Ashikin Abu Bakar and Nor Fadhilah Dzulkifli. "Slip effect on unsteady hybrid nanofluid flow over a stretching/shrinking surface." In *AIP Conference Proceedings*, vol. 2872, no. 1. AIP Publishing, 2023. <https://doi.org/10.1063/5.0162789>

- [15] Mahmood, Zafar, Khadija Rafique, Umar Khan, Magda Abd El-Rahman and Rabab Alharbi. "Analysis of mixed convective stagnation point flow of hybrid nanofluid over sheet with variable thermal conductivity and slip Conditions: A Model-Based study." *International Journal of Heat and Fluid Flow* 106 (2024): 109296. <https://doi.org/10.1016/j.ijheatfluidflow.2024.109296>
- [16] Afzal, Sidra, Mubashir Qayyum and Gilbert Chambashi. "Heat and mass transfer with entropy optimization in hybrid nanofluid using heat source and velocity slip: A Hamilton–Crosser approach." *Scientific Reports* 13, no. 1 (2023): 12392. <https://doi.org/10.1038/s41598-023-39176-5>
- [17] Hussain, Mohib, Muhammad Imran, Hassan Waqas, Taseer Muhammad and Sayed M. Eldin. "An efficient heat transfer analysis of MHD flow of hybrid nanofluid between two vertically rotating plates using Keller box scheme." *Case Studies in Thermal Engineering* 49 (2023): 103231. <https://doi.org/10.1016/j.csite.2023.103231>
- [18] Hartmann, J. and F. Lazarus. "Hg-dynamics II." *Theory of laminar flow of electrically conductive Liquids in a Homogeneous Magnetic Field* 15, no. 7 (1937).
- [19] Alqahtani, Aisha M., Khadija Rafique, Zafar Mahmood, Bushra R. Al-Sinan, Umar Khan and Ahmed M. Hassan. "MHD rotating flow over a stretching surface: The role of viscosity and aggregation of nanoparticles." *Heliyon* 9, no. 11 (2023). <https://doi.org/10.1016/j.heliyon.2023.e21107>
- [20] Sharma, Surbhi, Amit Dadheech, Amit Parmar, Jyoti Arora, Qasem Al-Mdallal and S. Saranya. "MHD micro polar fluid flow over a stretching surface with melting and slip effect." *Scientific reports* 13, no. 1 (2023): 10715. <https://doi.org/10.1038/s41598-023-36988-3>
- [21] Rafique, Khadija, Zafar Mahmood and Umar Khan. "Mathematical analysis of MHD hybrid nanofluid flow with variable viscosity and slip conditions over a stretching surface." *Materials Today Communications* 36 (2023): 106692. <https://doi.org/10.1016/j.mtcomm.2023.106692>
- [22] Nabwey, Hossam A., Ahmed M. Rashad, Waqar A. Khan, S. M. M. El-Kabeir and Shereen AbdElnaem. "Heat transfer in MHD flow of Carreau ternary-hybrid nanofluid over a curved surface stretched exponentially." *Frontiers in Physics* 11 (2023): 1212715. <https://doi.org/10.3389/fphy.2023.1212715>
- [23] Ragueb, Haroun, Antar Tahiri, Dounya Behnous, Belkacem Manser, Kamel Rachedi and Kacem Mansouri. "Irreversibilities and heat transfer in magnetohydrodynamic microchannel flow under differential heating." *International Communications in Heat and Mass Transfer* 149 (2023): 107155. <https://doi.org/10.1016/j.icheatmasstransfer.2023.107155>
- [24] Reddy, M. Gnaneswara and K. Venugopal Reddy. "Influence of Joule heating on MHD peristaltic flow of a nanofluid with compliant walls." *Procedia Engineering* 127 (2015): 1002-1009. <https://doi.org/10.1016/j.proeng.2015.11.449>
- [25] Ibrahim, Wubshet and Tezera Gizewu. "Stability analysis of dual solutions for mixed convection and thermal radiation with hybrid nanofluid flow past shrinking/stretching curved surface." *Scientific Reports* 13, no. 1 (2023): 21676. <https://doi.org/10.1038/s41598-023-48728-8>
- [26] Jayanthi, Senthil and Hari Niranjan. "Effects of Joule heating, viscous dissipation and activation energy on nanofluid flow induced by MHD on a vertical surface." *Symmetry* 15, no. 2 (2023): 314. <https://doi.org/10.3390/sym15020314>
- [27] Naseem, Tahir, Urooj Fatima, Mohammad Munir, Azeem Shahzad, Nasreen Kausar, Kottakkaran Sooppy Nisar, C. Ahamed Saleel and Mohamed Abbas. "Joule heating and viscous dissipation effects in hydromagnetized boundary layer flow with variable temperature." *Case Studies in Thermal Engineering* 35 (2022): 102083. <https://doi.org/10.1016/j.csite.2022.102083>
- [28] Hussain, Farooq, Mubbashar Nazeer, Abdullah Mengal, Asif Hussain and Syed Ali Raza Shah. "Numerical simulation of MHD two-dimensional flow incorporated with Joule heating and nonlinear thermal radiation." *ZAMM-Journal of Applied Mathematics and Mechanics/Zeitschrift für Angewandte Mathematik und Mechanik* 103, no. 6 (2023): e202100246. <https://doi.org/10.1002/zamm.202100246>
- [29] Ramesh, K., Arshad Riaz and Zahoor Ahmad Dar. "Simultaneous effects of MHD and Joule heating on the fundamental flows of a Casson liquid with slip boundaries." *Propulsion and Power Research* 10, no. 2 (2021): 118-129. <https://doi.org/10.1016/j.jprr.2021.05.002>
- [30] Asghar, Adnan, Yuan Ying Teh, Muhammad Javed Iqbal and Liaqat Ali. "Thermal characterization of hybrid nanofluid with impact of convective boundary layer flow and Joule heating law: Dual solutions case study." *Modern Physics Letters B* 38, no. 19 (2024): 2450158. <https://doi.org/10.1142/S0217984924501586>
- [31] Devi, SP Anjali and S. Suriya Uma Devi. "Numerical investigation of hydromagnetic hybrid Cu–Al₂O₃/water nanofluid flow over a permeable stretching sheet with suction." *International Journal of Nonlinear Sciences and Numerical Simulation* 17, no. 5 (2016): 249-257. <https://doi.org/10.1515/ijnsns-2016-0037>
- [32] Khashi'ie, Najiyah Safwa, Norihan Md Arifin and Ioan Pop. "Magnetohydrodynamics (MHD) boundary layer flow of hybrid nanofluid over a moving plate with Joule heating." *Alexandria Engineering Journal* 61, no. 3 (2022): 1938-1945. <https://doi.org/10.1016/j.aej.2021.07.032>

- [33] Anuar, Nur Syazana, Norfifah Bachok and Ioan Pop. "A stability analysis of solutions in boundary layer flow and heat transfer of carbon nanotubes over a moving plate with slip effect." *Energies* 11, no. 12 (2018): 3243. <https://doi.org/10.3390/en11123243>
- [34] Aladdin, Nur Adilah Liyana, Norfifah Bachok and I. Pop. "Cu-Al₂O₃/water hybrid nanofluid flow over a permeable moving surface in presence of hydromagnetic and suction effects." *Alexandria Engineering Journal* 59, no. 2 (2020): 657-666. <https://doi.org/10.1016/j.aej.2020.01.028>
- [35] Khan, Waqar A., Richard Culham and Rizwan Ul Haq. "Heat transfer analysis of MHD water functionalized carbon nanotube flow over a static/moving wedge." *Journal of Nanomaterials* 2015, no. 1 (2015): 934367. <https://doi.org/10.1155/2015/934367>